Waveguide Bragg Grating Filters

Ravindu Karunathilake

Bragg gratings filters are a fundamental component for achieving wavelength selective functionality in silicon photonics. In this report, the fundamental principles of designing a Bragg grating on silicon is presented. In addition, a practical filter design operating at 1550 nm is demonstrated. The proposed filter design was able to achieve a transmission of -52 dB with a bandwidth of 10 nm at 1550 nm.

The Bragg grating is an essential optical device created by periodic variation in effective refractive index along the propagation direction in a waveguide or an optical fiber core. [1] This index modulation is typically achieved by spatially alternating the material (such as in distributed Bragg reflectors lasers) or by changing the physical dimensions of a waveguide. Bragg gratings have found use in many optical devices such as semiconductor lasers, and sensors. The index modulation profile of these gratings induce a wavelength-selective functionality. As such, these devices are suited for optical filter design.

In this report, the theory of waveguide-based Bragg grating design will be covered. Afterwards, a practical filter, designed to operate at the telecommunication wavelength of 1550 nm will be presented. The report also includes the simulated optical response of the proposed design. The report concludes with a look at the practical fabrication considerations for the design.

Theory of Bragg Gratings

The periodic nature of the index profile results in a forward and backward travelling wave in the waveguide. These reflected waves (backward waves), interfere constructively in a narrow region centered on the Bragg wavelength (filter wavelength). [2] The relative phase of the reflected waves is determined by the grating period. The optical response of these periodic structures may be calculated based on Coupled Mode Theory (CMT).

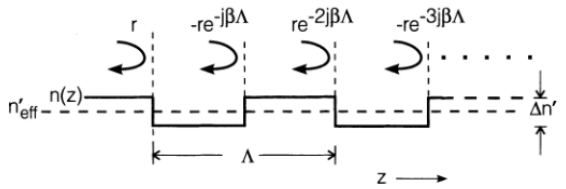

Fig. 1 | Square grating index profile. Illustration of a periodic index profile ($\boldsymbol{n(z)}$) in a corrugated waveguide with periodically varying effective index ($\boldsymbol{n'_{eff}}$). $\boldsymbol{\Lambda}$ is the grating period, and $\boldsymbol{r}$ is the field reflection coefficient. The arrows pointing in the $-z$ directions indicates the multiple distributed reflections throughout the waveguide grating.[2]

CMT assumes that eigenmodes of a coupled waveguide system can be represented by the guided modes of the individual waveguide (linear system). Furthermore, in the following derivations, the law of conservation of energy is employed. Based on previous work [2], the refractive index $n(z)$ for a periodic structure can be written as

$$n(z) = n(z + \Lambda) = n'_{eff} + \frac{4}{\pi}\frac{\Delta n'}{2}\cos(2\beta_0 z) \quad \textbf{(1)}$$

Where β_0 the Bragg waveguide propagation is constant, n'_{eff} is the average index value, and $\Delta n'/2$ is the amplitude of the periodic index variation. In the above derivation the transverse and lateral variations are neglected and the assumption of rectangular index variation is taken. The phase detune

(δ) originating due to the periodic index perturbation can be modeled as

$$\delta = \beta_0 - \frac{M\pi}{\Lambda} \quad \textbf{(2)}$$

For maximum reflection at the Bragg wavelength (λ_0), the phase detune is zero. Where M is the period order. For the proceeding formulations, a first-order structure with M = 1 will be assumed. From equation 2, by setting $\delta = 0$, and knowing $\beta_0 = 2\pi n'_{eff}/\lambda_0$ the necessary period of the index perturbation is determined

$$\Lambda = \frac{\lambda_0}{2n'_{eff}} \quad \textbf{(3)}$$

As before, neglecting all transverse and lateral field variations the propagating electric field is defined by [2]

$$\frac{dE(z)}{dz} + [n(z)k]^2 E(z) = 0 \quad \textbf{(4)}$$

Where $k = 2\pi/\lambda$ is the free-space propagation constant for wavelength λ. Expanding the second term in equation 4 and neglecting high order $(\Delta n)^2$ terms yields

$$[n(z)k]^2 = \beta^2 + 4\beta\kappa cos(2\beta_0 z) \quad \textbf{(5)}$$

Where β is the propagation constant at wavelength λ and κ is the coupling coefficient given by

$$\kappa = \frac{2\Delta n}{\lambda} \quad \textbf{(6)}$$

Considering wavelengths λ near the Bragg wavelength λ_0, the field $E(z)$ may be decomposed into the right- and left-propagating waves: [2]

$$E(z) = R(z)e^{-j\beta_0 z} + S(z)e^{j\beta_0 z} \quad \textbf{(7)}$$

By substituting equation (7) and (5) into (4) and neglecting higher-order differential terms yield the couple-mode equations (CMEs) [2]:

$$\frac{dR(z)}{dz} + j(\beta - \beta_0)R(z) = -j\kappa S(z) \quad \textbf{(8)}$$

$$\frac{dS(z)}{dz} - j(\beta - \beta_0)S(z) = -j\kappa R(z) \quad \textbf{(9)}$$

The general solutions to these coupled, linear, first-order differential equations are given by [2]

$$R(z) = \left[\cosh(\gamma z) - j\frac{\Delta\beta}{\gamma}\sinh(\gamma z)\right]R(0) - j\frac{\kappa}{\gamma}\sinh(\gamma z)S(0) \quad \textbf{(10)}$$

$$S(z) = \left[\cosh(\gamma z) + j\frac{\Delta\beta}{\gamma}\sinh(\gamma z)\right]S(0) + j\frac{\kappa}{\gamma}\sinh(\gamma z)R(0) \quad \textbf{(11)}$$

Where $\gamma^2 = \kappa^2 - \Delta\beta^2$ and $\Delta\beta = \beta - \beta_0$ is the propagation constant off-set from λ_0 with $\Delta\beta << \beta_0$. The reflectivity (R) in the stop-band ($\Delta\beta^2 < \kappa^2$) for Bragg grating of length L is given by:

$$R_{stop} = \frac{|\kappa|^2 \sinh^2(|\gamma|L)}{|\gamma|^2 \cosh^2(|\gamma|L) + \Delta\beta^2 \sinh^2(|\gamma|L)} \quad \textbf{(12)}$$

The reflectivity (R) in the passband ($\Delta\beta^2 \geq \kappa^2$) for Bragg grating of length L is given by:

$$R_{pass} = \frac{|\kappa|^2 \sin^2(\gamma L)}{\gamma^2 \cos^2(\gamma L) + \Delta\beta^2 \sin^2(\gamma L)} \quad \textbf{(13)}$$

From equation 12, the maximum peak power reflectivity occurs when $\Delta\beta = 0$:

$$R_{peak} = \tanh^2(\kappa L) \quad \textbf{(14)}$$

In addition the bandwidth of Bragg grating is defined as [3]

$$\Delta\lambda = \frac{\lambda_0^2}{\pi n_g}\sqrt{\kappa^2 + (\pi/L)^2} \quad \textbf{(15)}$$

For sufficiently long gratings ($\kappa >> \pi/L$), equation 15 may be simplified to:

$$\Delta\lambda = \frac{\lambda_0^2 \kappa}{\pi n_g} \quad \textbf{(16)}$$

Where the group index (n_g) defined as

$$n_g = n_{eff} - \lambda \frac{dn_{eff}}{d\lambda} \quad \textbf{(17)}$$

Note however, the bandwidth defined in equation 15 is not the 3dB bandwidth, but rather the bandwidth between the first nulls around the main reflection peak.

Filter Design

For Bragg grating designs, in general, a single-mode (TE) waveguide is preferred. [3] Thus, by adhering to Si thickness in standard CMOS foundry compatible SOI wafers, the width (Fig. 2) of the waveguide must be determined.

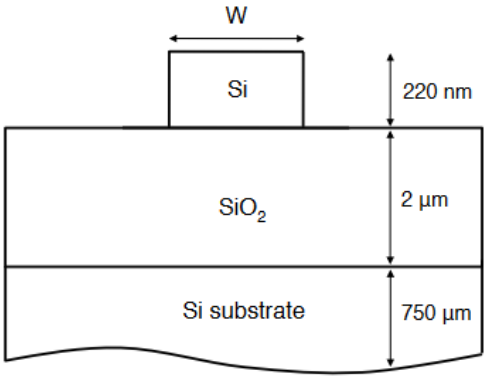

Fig. 2 | Standard SOI wafer. The standard dimensions of a commercially available SOI wafer. The buried oxide layer must be of sufficient thickness to isolate the top Si waveguide from the Si substrate.[3]

In addition, an oxide cladding for the Bragg grating is used. Oxide cladding is typically used to protect the waveguide structure from oxidation, and to permit metal interconnects above the waveguide.[4] Consequently, adding the cladding has the effect of symmetric intensity distribution for TM mode (Figure 4). Given these practical design constraints, the effective index of the waveguide was determined via parameter sweep in Lumerical MODE solutions. First, however, the ideal width of the waveguide for single mode operation must be chosen. As such, a width parameter sweep (at 1550 nm wavelength) in Lumerical MODE Solutions was conducted: the results of which is shown in Figure 3.

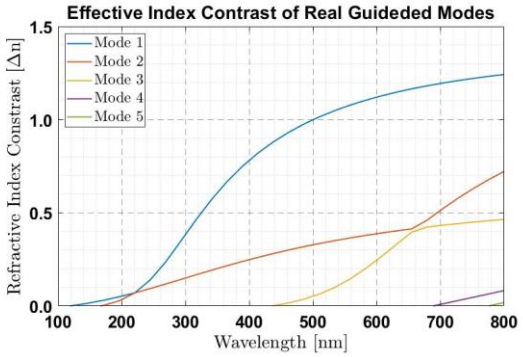

Fig.3 | Supported guided modes in a waveguide. The plot illustrates that there are various number of supported modes for the waveguide depending on the waveguide width. The refractive index contrast is defined as the refractive index difference between the effective index of any given mode and the SiO_2 refractive index (~1.444 @ 1550 nm).

Based on results from above, a waveguide width of 500 nm is chosen for the Bragg grating design. A width of 500 nm is chosen for two reasons: ease of manufacturing, and the relatively small intensity confinement for the second TE mode. Figure 4 shows the field intensity confinement for the three possible guides modes for a width of 500 nm: fundamental TE mode (blue line in Figure 3), fundamental TM mode (orange line in Figure 3), and second TE mode (yellow line in Figure 3). As can be seen from the bottom plot of Figure 4, the choice of 500 nm width for the waveguide is justified given the field intensity distribution for the second TE mode is mostly along the sidewalls on the waveguide. Therefore, the effective index is small for this mode compared to the fundamental

TE mode and thus, results in higher propagation loss.

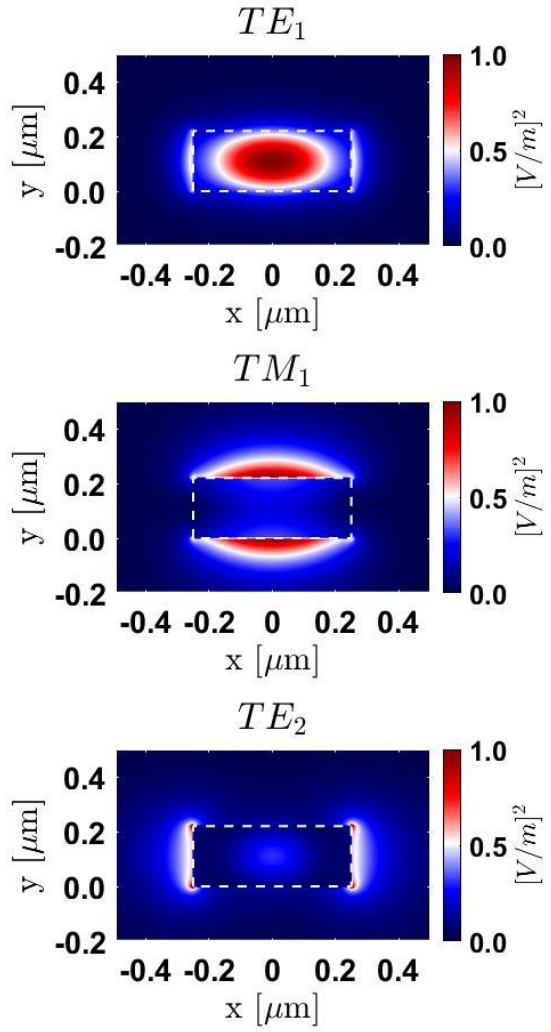

Fig. 4 | Field intensity plot for guided modes. The top field plot showcases the field distribution for the fundamental TE mode for a waveguide of width 500 nm. Likewise, the middle and bottom plots displays the field intensity for the fundamental TM and second TE mode, respectively. Note, SiO_2 substrate is present for y < 0 μm (not shown in the dotted white structural outline).

Having determined an appropriate width for the waveguide the effective index for the three guided modes where calculated. The calculated effective indices, group indices, and loss for the modes are summarized in table 1 below. Using this information and the data from table 2, the grating period can be calculated using the Bragg condition (eq. 3).

Mode #	n_{eff}	n_g	Loss (dB/cm)
1	2.445198	4.208971	0.00044982
2	1.770684	3.737372	0.00025060
3	1.494712	2.400141	0.00012373

Table 1 | Calculated effective indices for the input/output waveguides. The table summarizes the effective index, group index and loss calculated for the three guided modes present in a waveguide with a width of 500 nm. The calculations were performed using Lumerical MODE Solutions.

Based on the data presented in table 1 for the fundamental TE mode, the period of the Bragg grating is calculated to be $316.948\,nm$. The next parameter to be determined is the corrugation depth, which determined the coupling coefficient and in turn the bandwidth of the grating in the stopband. To achieve sub-nanometer bandwidth using strip waveguides require corrugation width of less than 10 nm. [4] Given the fabrication limitation, this level of performance is challenging to achieve. Therefore, a modest bandwidth of 20 nm will be targeted. Given this design bandwidth, the coupling coefficient (κ) is determined to be $1.04223 \times 10^{-4}\,nm^{-1}$ from equation 15. Knowing the coupling coefficient, the required index contrast between the periodic variations (Δn) is determined to be 0.08077 from equation 6 at the Bragg wavelength. Based on simulation results (table 2) the ideal corrugation depth to achieve this index contrast is 25 nm.

Segment Width (nm)	n_{eff}
475	2.400218
525	2.479579

Table 2 | Calculated effective indices for the Bragg grating segments. The table summarizes the effective index of the fundamental TE mode for the two main waveguide segments in a Bragg waveguide filter. The calculations were performed using Lumerical MODE Solutions.

Based on the determined values for the period and corrugation depth, a Lumerical EigenMode Expansion (EME) simulation was conducted to obtain the optical response of the Bragg grating structure (Fig. 5). From equation 3, it is easily observed that the period of the Bragg grating is directly proportional to the Bragg wavelength. From the results presented in Figure 5, when the period is increased (decreased), the Bragg wavelength red shifts (blue shifts). Even a minor period shift of 2 nm can shift the operational wavelength as much as 5 nm. This suggests, the proposed design is highly sensitive to fabrication tolerances.

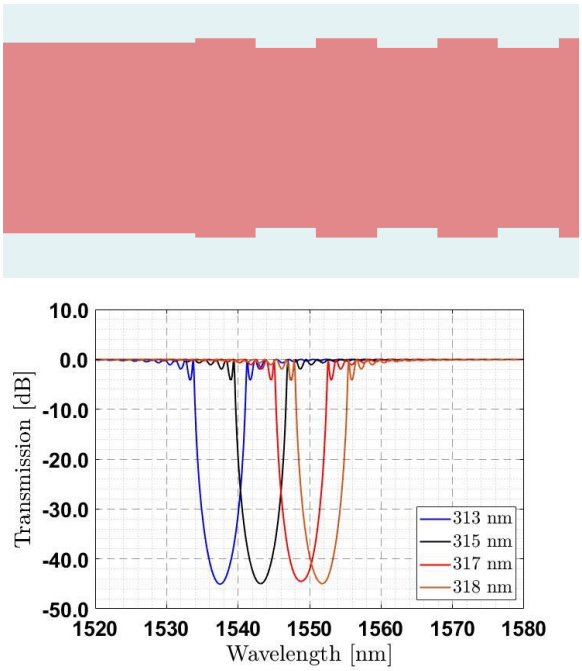

Fig. 5 | EME Bragg grating optical response. Top diagram illustrated the simulated Bragg grating structure with a period of 317 nm, a corrugation width of 25 nm and an overall structural length of 158.5 μm. The plot illustrates the simulated transmission spectra for Bragg gratings with different periods (500 grating periods).

Furthermore, for the case of period of 317 nm (designed value), the response of the Bragg grating is not centered on 1550 nm as expected. This suggests there might be a sight miscalculation with regards to the effective index of the fundamental TE mode. In addition, the calculated bandwidth of 20 nm (as defined in equation 15) with a corrugation width of 25 nm was not achieved. Based on the results presented in Figure 5, the bandwidth was calculated to be ~8 nm. This suggests that the coupling coefficient is lower than the designed value. Additionally, the EME wavelength sweep tool might have introduced some error due to silicon material dispersion. Therefore, to obtain more accurate results, a 3D Lumerical Finite Difference Time Domain (FDTD) simulation with 280 grating period was run. The results of which can be seen in Figure 6 below.

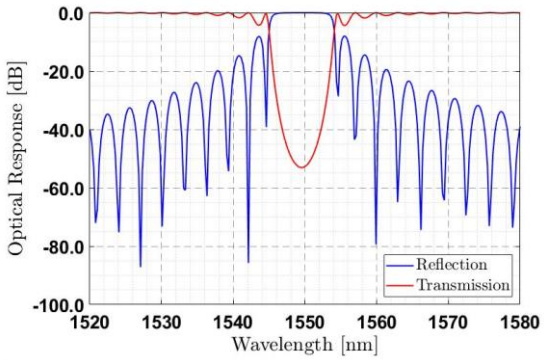

Fig. 6 | FDTD optical response. The simulated optical response of a Bragg grating for a period of 317 nm. The device shows -52 dB power transmission at the design wavelength of 1550 nm with a bandwidth (between the first nulls) of ~10 nm. The simulated device contained 280 grating periods (~89 μm).

Based on the FDTD results, the bandwidth of the proposed Bragg grating is ~10 nm: approximately half of the design bandwidth of 20 nm. However, from a performance perspective, a narrower bandwidth is preferred for a filter. As mentioned before, the derivation of bandwidth in equation 15 is for the first nulls around the main reflection peak. However, this derivation did not take into account material loss. Therefore, the discrepancy of bandwidth could be the result of this approximation as the second term under the square root of equation 15 is de-

pendent on the propagation constant deviation, $\Delta\beta$. The losses can be accounted by replacing $\Delta\beta$ by $\Delta\beta - j\alpha_o$ [3], where α_o is the field loss coefficient.

Fabrication Considerations

There are number of factors that must be considered when fabricating the proposed Bragg grating design. For instance, it is evident from equation 14, as the length of Bragg grating is increased, the peak reflectivity at the Bragg wavelength approach unity. In fabricating these large devices non-uniformity becomes a concern as variations in width and thickness is introduced. One solutions is to design long Bragg gratings inside a small area by designing spiral Bragg gratings. In addition, the given design contains high aspect ratio geometries, which are challenging to manufacture. In practical fabrication process, the square corrugations are likely to be fabricated with soft corners. Since the design is highly reliant on the propagating mode in these corrugation segments, the device is likely to deviate from the designed operation. The issue may be remedied by introducing empirical measurement data into the device design work flow or alternatively, rely on advanced lithography simulations to simulate the fabrication of the device.

Summary

The report focused on the fundamental theory of designing Bragg waveguide filters using couple mode theory equations. A practical design of one such device operating at 1550 nm was presented. For practical purposes, the proposed device was designed based on a commercially available SOI wafer with a 220 nm Si layer. Based on simulation results from Lumerical (photonic simulation software), the proposed design was able to achieve a filter transmission response of -52 dB with a bandwidth of 10 nm at 1550 nm. Given the high-aspect ratio geometries and the size of the proposed design, there is considerable sensitivity to fabrication errors. Thus, an iterative design process with the integration of empirical or simulated fabrication data is needed for the optimal design of the device. Furthermore, integrating a heater (thermo-optic effect) or a PN-junction (plasma effect) may be needed to further tune the response of the device post-fabrication.

References

1. Zhang, W. & Yao, J. A fully reconfigurable waveguide Bragg grating for programmable photonic signal processing. *Nat. Commun.* 9, 1396 (2018).
2. Buus, J., Amann, M.-C., Blumenthal, D. J. & Amann, M.-C. *Tunable laser diodes and related optical sources*. (John Wiley & Sons, 2005).
3. Wang, X. Silicon Photonic Waveguide Bragg Gratings. 182.
4. Chrostowski, L. & Hochberg, M. *Silicon Photonics Design*. (Cambridge University Press, 2015). doi:10.1017/CBO9781316084168.